Entanglement Witnessing: Neural Network Optimization and Experimental Realization

Oscar Scholin*,†, Richard Zheng†, Alec Roberson†, and Theresa W. Lynn†
†Department of Physics, Harvey Mudd College
*Department of Physics, Pomona College

Introduction

Entanglement is a unique and central phenomenon of quantum mechanics. This persistent correlation between the properties of a pair of particles can be harnessed in algorithms both in secure communication, such as super dense coding, and in computation, e.g. Grover's search. The ability to quickly and accurately verify entanglement between particles, therefore, is key to the quantum information revolution. We verify entanglement by measuring states in different bases and then calculating statistical correlations between measurements on the two particles. Riccardi et al. [1] define a set of 6 entanglement witnesses $\{W\}$, which are operators for which a negative expectation value verifies entanglement and all separable (i.e., non-entangled) states have a non-negative expectation value, and have direct application for photonics systems. Last year's team [5] extend their work to include 9 more $\{W'\}$, grouped into three "triplets" based on the local measurements they require.

Conclusions

1. Our neural network is able to predict up to 84.9% accurately the optimal triplet based on a set of nine input measurements at a 0 concurrence threshold for states with $W \geq 0$ and $W'_{\min} < 0$, which is a 4.0% increase from previous work.
2. We have successful experimental results for a class of states, $E_0(\eta, \chi) = \cos\eta|\Psi^+\rangle + \sin\eta e^{i\chi}|\Psi^-\rangle$, that $\{W\}$ cannot detect but $\{W'\}$ does.
3. All our code is available on our GitHub repository: `https://github.com/Lynn-Quantum-Optics/Summer-2023`.

Theoretical Neural Network

Last year's team [5] define a group of nine entanglement witness $\{W'\}$, which are grouped into sets of three additional measurements called "triplets" W'_{t_X} for $X \in [1, 2, 3]$. We optimize the entanglement verification process by determining which of the three "triplets" to choose. We consider three primary models (see Table 2): "Population", an analytical method developed by Eritas Yang [4], "NN2" the previous best-performing neural network by Becca Verghese and Laney Goldman [3], and "NN5" our current model.
We trained NN5 on 80% of 1.2×10^6 states and used the other 20% validation data for hyperparameter sweeping. We separately tested the model, as well as the previous, on a new set of 1.2×10^5 states, which satisfy $\min W \geq 0$ and $\min W'_{t_X} < 0$, where the minimum is applied within each triplet (which reduces an unrestricted dataset down to 30.2% of initial size). We generated random states in the style of [2], which involved a random simplex for the diagonal elements and a combination of 6 unitaries to provide the mixedness. Prior to W and W' filtration, 67.6% of data is entangled—this is the data we report undetected fractions on in Figure 1.

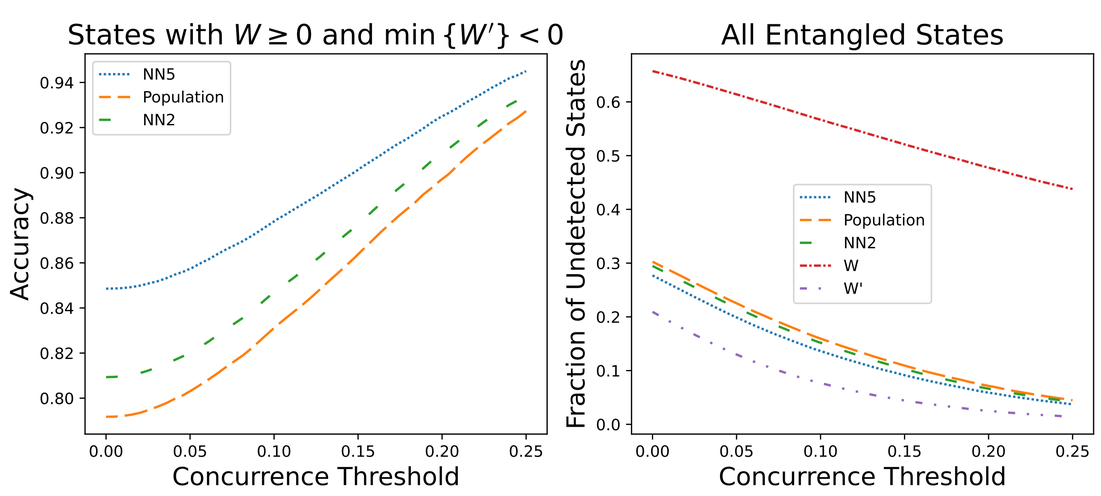

Figure 1: Performance comparison of predictive models as a function of coherence threshold, as described in table 2. Strength of entanglement required for witness selection increases in the positive x direction. Left: compares the accuracy on states satisfying $\min W \geq 0$ and $\min W'_{t_X} < 0$. Right: the fraction of states undetected both by W and all W' in addition to the models on entangled states with no prior W and W' restriction.

Model	Input Params	Architecture	Acc., UF
Pop.	D_{HV}, D_{DA}, D_{RL}	Argmax of input	79.2%, 30.3%
NN2	HH, HV, VH, VV, DD, DA, AD, DD, RR, RL, LR, LL	2 hidden layer NN	80.9%, 29.5%
NN5	HH, HV, VV, DD, DA, DD, RR, RL, LL	5 hidden layer NN	84.9%, 27.7%

Table 1: Summary of model performance as a function of concurrence threshold. Acc. is the accuracy when tested on a restricted 1.2×10^5 unseen states for which $\min W \geq 0$ and $\min W'_{t_X} < 0$, and UF is the undetected fraction of states on 2.7×10^5 unseen entangled states. XY is the probability of measuring X state for the left and Y for the right particle. Also, $D_{XY} = 0.5 - (XX + YY)$. NN is neural network.

Model	Sizes and activation	Learning rate / Opt.	Loss
NN2	7 (ReLu), 5 (Softmax)	10^{-2}, Adam	$y \cdot \hat{y}$
NN5	200 (ReLu) $\times5$	10^{-3}, Adam	$-\hat{y} \cdot \log y$

Table 2: Summary of neural network structures, by [3] (NN2) and this work (NN5). Size is number of neurons per layer, and in paranethesis is the activation function. Opt. stands for optimizer, Loss is the loss function. y is the predicted output probability vector (using the Sigmoid activation function), and $\hat{y}$ is the target multi-hot vector.

Experimental Data

Consider the experimental setup shown in figure 2. Our results for the state $E_0(\eta, \chi) = \cos\eta|\Psi^+\rangle + \sin\eta\, e^{i\chi}|\Psi^-\rangle$, where $|\Psi^\pm\rangle = |HV\rangle \pm |VH\rangle$, are shown in figure 3 for $\eta = 30°, 45°$ and χ swept from 0 to $\frac{\pi}{2}$. The entanglement of these states is not detectable by $\{W\}$ but is by $\{W'\}$ theoretically, and we verify this result experimentally.

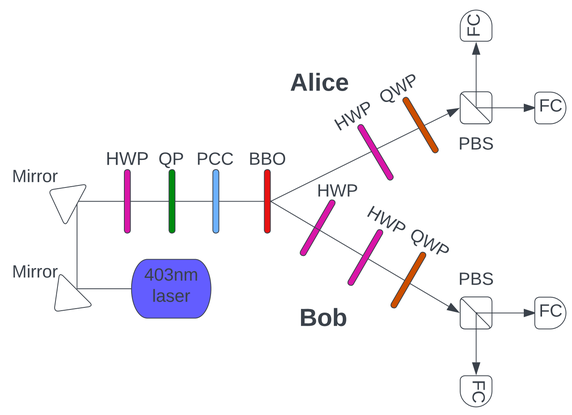

Figure 2: Illustration of experimental setup. HWP is half waveplate, QWP quarter waveplate, QP quartz plate, and PCC precompensation crystal. The HWP, QP, PCC, allow for initial state creation of the form $\sin^2(2\theta)|H\rangle + \cos^2(2\theta)e^{i\phi}|V\rangle$, the BBO induces spontaneous parametric downconversion (SPDC), and the first HWP on the path labeled "Bob" allows the second photon polarization to be phase-shifted by π. Then, a HWP and a QWP on each of Bob and the other path Alice allow for measurement configuration, where finally the light enters a polarizing beam splitter (PBS) and enters detectors.

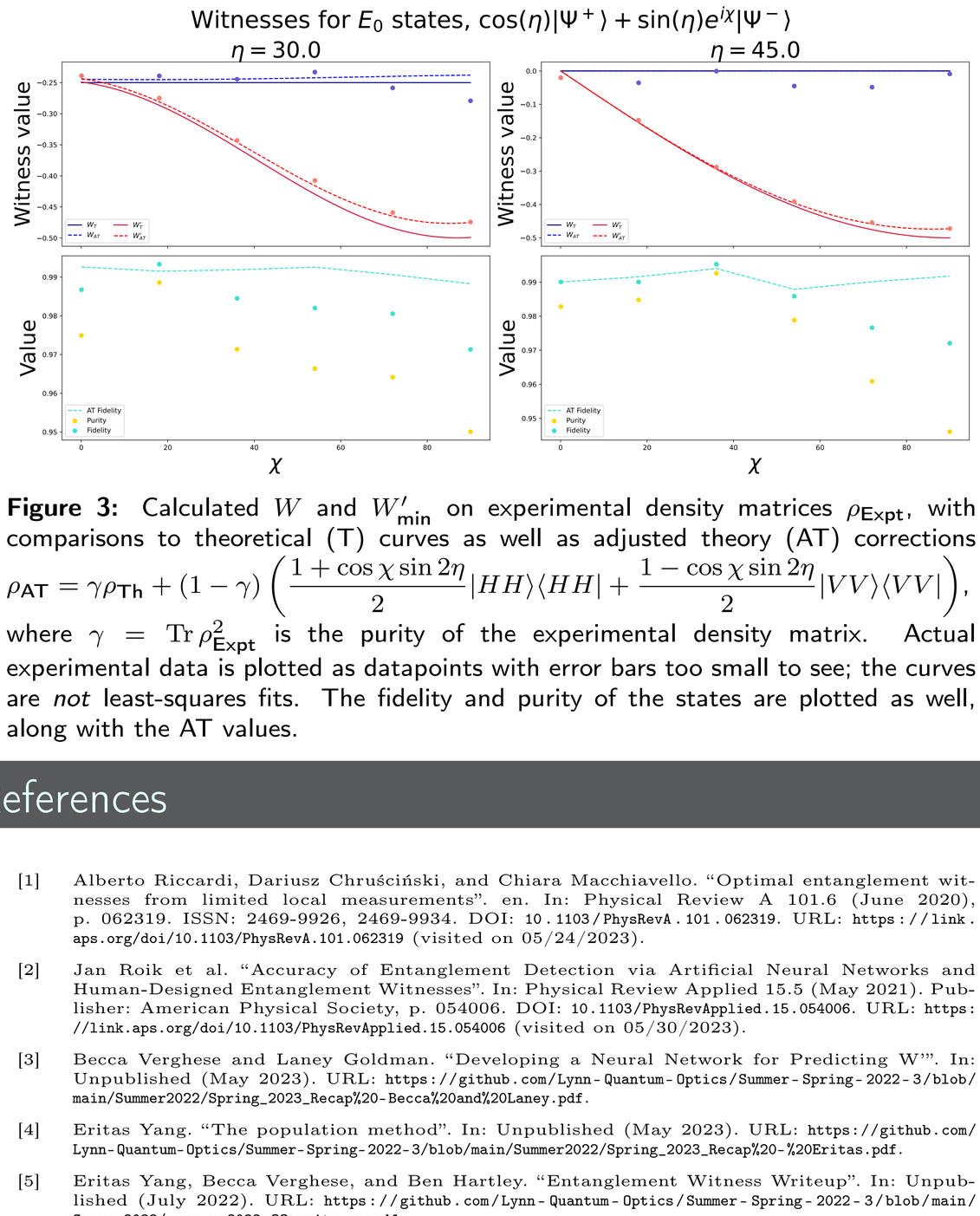

Figure 3: Calculated W and $W'_{\min}$ on experimental density matrices ρ_{Expt}, with comparisons to theoretical (T) curves as well as adjusted theory (AT) corrections $\rho_{\text{AT}} = \gamma\rho_{\text{Th}} + (1-\gamma)\left(\frac{1+\cos\chi\sin2\eta}{2}|HH\rangle\langle HH| + \frac{1-\cos\chi\sin2\eta}{2}|VV\rangle\langle VV|\right)$, where $\gamma = \operatorname{Tr}\rho^2_{\text{Expt}}$ is the purity of the experimental density matrix. Actual experimental data is plotted as datapoints with error bars too small to see; the curves are *not* least-squares fits. The fidelity and purity of the states are plotted as well, along with the AT values.

Acknowledgements

We thank the Harvey Mudd Physics Summer Research Fund (PSRF).

References

[1] Alberto Riccardi, Dariusz Chruściński, and Chiara Macchiavello. "Optimal entanglement witnesses from limited local measurements". en. In: Physical Review A 101.6 (June 2020), p. 062319. ISSN: 2469-9926, 2469-9934. DOI: 10.1103/PhysRevA.101.062319. URL: https://link.aps.org/doi/10.1103/PhysRevA.101.062319 (visited on 05/24/2023).

[2] Jan Roik et al. "Accuracy of Entanglement Detection via Artificial Neural Networks and Human-Designed Entanglement Witnesses". In: Physical Review Applied 15.5 (May 2021). Publisher: American Physical Society, p. 054006. DOI: 10.1103/PhysRevApplied.15.054006. URL: https://link.aps.org/doi/10.1103/PhysRevApplied.15.054006 (visited on 05/30/2023).

[3] Becca Verghese and Laney Goldman. "Developing a Neural Network for Predicting W"". In: Unpublished (May 2023). URL: https://github.com/Lynn-Quantum-Optics/Summer-Spring-2022-3/blob/main/Summer2022/Spring_2023_Recap%20-Becca%20and%20Laney.pdf.

[4] Eritas Yang. "The population method". In: Unpublished (May 2023). URL: https://github.com/Lynn-Quantum-Optics/Summer-Spring-2022-3/blob/main/Summer2022/Spring_2023_Recap%20-%20Eritas.pdf.

[5] Eritas Yang, Becca Verghese, and Ben Hartley. "Entanglement Witness Writeup". In: Unpublished (July 2022). URL: https://github.com/Lynn-Quantum-Optics/Summer-Spring-2022-3/blob/main/Summer2022/summer-2022-QO_write_up.pdf.